Universidade de São Paulo

Biblioteca Digital da Produção Intelectual - BDPI

Departamento de Física e Ciência Interdisciplinar - IFSC/FCI

Artigos e Materiais de Revistas Científicas - IFSC/FCM

2011-12

De-aggregation of a polyfluorene derivative in clay nanocomposites: a photophysical study

Macromolecular Nanotechnology

De-aggregation of a polyfluorene derivative in clay nanocomposites: A photophysical study

José Roberto Tozoni [a,*], Francisco Eduardo Gontigo Guimarães [b], Teresa Dib Zambon Atvars [c], Bruno Nowacki [d], Alexandre Marlleta [a], Leni Akcelrud [d,*], Tito José Bonagamba [b,*]

[a] Instituto de Física, Universidade Federal de Uberlândia, P.O. Box 593, Uberlândia, 38400-902 Minas Gerais, Brazil
[b] Instituto de Física de São Carlos, Universidade de São Paulo, P.O. Box 369, São Carlos, 13560-970 São Paulo, Brazil
[c] Chemistry Institute, State University of Campinas (Unicamp), P.O. Box 6154, Campinas, 13084-971 São Paulo, Brazil
[d] Laboratório de Polímeros Paulo Escarpa (LaPPS) UFPR, Universidade Federal do Paraná, P.O. Box 19081, Curitiba, 81531-990 Paraná, Brazil

ARTICLE INFO

ABSTRACT

The de-aggregation of a very luminescent polyfluorene derivative poly(9,9-di-hexylfluorenediyl divinylene-alt-1,4-phenylenevinylene), which has a high tendency to π-stacking aggregation was achieved through the interaction of the polymer with clay in clay/polymer nanocomposites. The mixing of diluted toluene polymer solutions with kaolinite was enough to promote the de-aggregation, even without the indication of polymer intercalation, indicating that the polymer de-aggregation was obtained due to its interactions with clay platelet surfaces. The photoluminescence observed for the dispersed polymer on clays showed an increase in intensity and a blue-shift of the photoluminescence, when compared with pure pristine material in thin film form. The results presented bring the possibility to produce more efficient polymer based devices and to carry single molecule studies using nanocomposite film formation.

© 2011 Elsevier Ltd. All rights reserved.

1. Introduction

Conjugated polymers have received great attention in the semiconductor industry due to its technological interest for innovations in electroluminescent and photovoltaic devices and sensors, among others [1–8]. The electronic properties of these materials are controlled by their band gaps, which in turn depends on chemical structure, effective conjugation length, macromolecular conformation, and inter- and intra-chain association tendency [3,4,9,10]. The latter has a strong influence on energy migration, charge transport, and efficiency quantum yield [3,4,9,10], and different approaches can be used to avoid or to reduce them. One involves chemical changes of polymer chemical structure by inserting inert spacers, meta-linkages, or lateral branches [3,4,9,10]. However, these chemical changes also modify the band gap and electrical properties of the material [3,4,9,10]. Another approach involves the blending of the conjugated polymer, which combines the physical–chemical properties of the components to enhance specific characteristics. Electroluminescence properties, for example, change dramatically through de-aggregation with a high charge transport improvement [4,9–11]. The reason for this improvement has been attributed to the formation of heterojunctions, which create percolation channels for charge transport [4,9–11]. However, in addition to heterojunctions, other morphological changes are also modified [4,9–11]. In particular, partial polymer de-aggregation has been observed and may play some role in the device performance [4,9–11]. Nevertheless, due to the complexity of the solid state morphology involving multiphasic systems, either produced by the size distribution of domains or by the large

conformational distribution of the chains, both photo and electroluminescent properties are complex and broad bands are usually observed [4,9–11]. Thus, identifying de-aggregation of polymer chains in blends is not an easy task, unless the aggregate emission is intense (which normally is not the case) and strongly red-shifted compared to the isolated emission. Single molecule experiments are particularly important methodologies to study the emission of individual molecules [12–14]. When a representative set of molecules is analyzed, the entire spectrum of non-aggregate molecules can be obtained by adding every single molecule spectrum [12,14]. That method is based on the dilution of the luminescent polymer in an inert matrix and recording the emission (or time resolved spectroscopy) of several specific pixels of the sample [12,14].

Chain isolation is a very difficult task in conjugated polymers due the strong interchain interaction [15,16]. Thus, several attempts have reported to get isolate chains, mostly of them using inert polymers (poly(methyl methacrylate) and polystyrene) or materials with mesoporous structures [15,16]. But even though for these systems, judicious experimental conditions must be implemented as assure the chain isolation.

In a previous paper, we have shown that the capability of an inert polymer to dilute conjugate polymer is strongly dependent on the polymer–polymer interactions [17]. The polymer studied was a polyfluorene derivative, namely poly[(9,9-dihexyl-9H-fluorene-2,7-diyl)-1,2-ethenediyl-1,4-phenylene-1,2-ethenediyl] (LaPPS16) [18], which undergoes larger de-aggregation in poly(isobutyl methacrylate) than in other poly(alkyl methacrylate) matrices [17]. Therefore, the proposal of the development new systems for polymer de-aggregation is an important challenge for several different applications [1–18].

Based in the previous results [17], we extended the de-aggregation studies using clays and LaPPS16 as chromophore. The de-aggregation was observed through the polyfluorene adsorption on clay surfaces, making a kind of photoluminescent clay/polymer nanocomposite. Clays have being used for several purposes imparting interesting new properties to the composite: better mechanical and thermal stability, improved frame retardant features, and greater photostability, among others [19–25]. Clays have nanometric dimensions (∼1 to 5000 nm) and high surface areas (∼7 to 800 m^2/g) [19] where the polymers can be adsorbed. There are several ways to prepare clay/polymer nanocomposites [19,25], including sorbate adsorption on the clay surface by casting and further solvent evaporation [19,23], and in situ polymerization on the particle surface or interlayer space [20,25]. The low affinity between the emissive polymer (hydrophobic) and the clay (hydrophilic and hydrophobic surfaces) is one of the main challenges to overcome in preparing clay/polymer nanocomposites. In general, this is the main difficult to achieve the compatibility between organic and inorganic components [19,25]. Other important parameters are concerned to (i) the sorbed polymer (molecular weight, chemical nature of the repeating units, chain structure and conformation, and ability to undergo specific interactions), (ii) the clay (surface area, size cavities, surface hydrophylicity, and surface charges), and (iii) the solvent (polarity, pH, and solvation parameters) [19–25].

In the present case, the mixture of the low concentrated conjugated polymer toluene solution with the non-treated clay was enough to promote the de-aggregation of LaPPS16 through the polymer absorption on the clay surfaces. The clay used for this study was kaolinite, a kind of aluminum silicate hydrate (KAO, Al$_2$Si$_2$O$_5$(OH)$_4$). This clay has about 7–30 m^2/g of surface area and belongs to the 1:1 clay mineral group [19]. The kaolinite structure is formed by both tetrahedral silica lamellar layers (more hydrophobic) and octahedral alumina lamellar layers (more hydrophilic) [19]. These connected layers, presenting both hydrophilicity and hydrophobicity, allow KAO to be well-dispersed in solvents like toluene, a good solvent also for polyfluorenes, including LaPPS16 [26].

The polymer de-aggregation was followed by steady state photoluminescence spectroscopy, a very sensitive technique based on the differences of the spectral profile and intensity of the emission from isolated and aggregate species [27–29].

2. Experimental

2.1. Materials

LaPPS16 was synthesized via Wittig condensation between 2,7-bis(bromomethyl)-9,9′-di-n-hexylfluorene and 2,7-bis[(p-triphenyl phosphonium) methyl]-9,9′-di-n-hexylfluorene dibromide as described elsewhere [16].

The clay (KAO) was purchased from Kanto Chemical Co. Inc. Tokyo Japan, and was used as received. The product name is Kaolin, it is an aluminum silicate hydrate. It is a white powder, insoluble in water and organic solvents, with chemical composition [Al2Si4O10(OH)2]·5SiO2, data provided by the manufacturer. Kaolinite is the main component in Kaolin but minor impurities, such as illite, muscovite and halloysite, may also be present. In the product used the impurities are in the range of 0.1%, chloride and iron as the main elements present, data provided by the manufacturer. Toluene PA was purchased from Aldrich.

2.2. Sample preparation

The KAO powder is formed by nanometric particles that showed plate structure with hexagonal outlines. Some plates stack together forming a vermicular structure [30]. It disperses in toluene when the solution is mechanically stirred. Samples were prepared mixing KAO, polymer, and toluene, the mixtures were then ultrasonicated and mechanically stirred. In the toluene/clay/polymer dispersion the solution is hazy due to the light scattering by clay particles and its color is yellow due to the blue-light absorption by the polymer. After the drying of the toluene/clay/polymer dispersion, the clay/polymer blend forms a yellow pale powder.

Four samples were prepared, keeping the clay concentration constant and varying the polymer concentration, as follows: clay (200 mg), toluene (40 mL), and 1 mL of polymer/toluene solution at 0.1, 0.2, 0.3, and 0.4 mg/mL,

Table 1
Sample labeling and processing conditions of KAO clay, polymer LaPPS16, and clay/polymer nanocomposites.

Label	Sample	Sonification (15 min)	Mechanical stirring (15 min)
Pure-KAO	Pure KAO as-received	–	–
Toluene-KAO	KAO + toluene	1×	1×
Toluene-polymer	LaPPS16 + toluene (4.7 mg/mL)	1×	–
Film-polymer	LaPPS16 spin coated film	1×	–
KAO-polymer 1	clay/polymer (2000/1 w/w)	1×	1×
KAO-polymer 2	clay/polymer (2000/2 w/w)	1×	1×
KAO-polymer 3	clay/polymer (2000/3 w/w)	1×	1×
KAO-polymer 4	clay/polymer (2000/4 w/w)	1×	1×
KAO-polymer 5	clay/polymer (2000/2 w/w)	5×	5×

corresponding to clay/polymer ratios 2000/1, 2000/2, 2000/3, and 2000/4 (w/w). Each mixture was sonicated during 15 min, mechanically stirred further 15 min and, finally, dried in ambient environment until complete toluene removal. For comparison purposes four additional samples were prepared: the first one was a spin coated film of the pure polymer diluted in toluene at 50.00 µmol L^{-1} on a glass substrate with a speed of 300 rpm for 2 min, a second one consisted of a solution of LaPPS16 in toluene at 4.7 µmol L^{-1}, a third was a solution of clay/toluene (clay (200 mg) and toluene (40 mL)), which was sonicated during 15 min, mechanically stirred further 15 min and dried in ambient environment until complete toluene removal, and a fourth was a KAO/LaPPS16 sample prepared by five sequential sonication steps (15 min)/mechanically stirring (15 min) cycles of a dispersion of KAO/toluene (200 mg/40 mL) and 1 mL of a toluene LaPPS16 solution at 0.2 mg/mL.

Table 1 describes those samples and their processing conditions.

2.3. Wide-angle X-ray diffraction (WAXD)

WAXD studies were performed using a Rigaku Rotaflex RU 200B instrument (Cu Kα radiation, λ = 1.5418 Å). WAXD measurements were carried out for three KAO samples: pure (as received), diluted in toluene, and diluted in a solution of toluene and polyfluorene 2000/2 (KAO-polymer 5). In the case of the KAO diluted in toluene, it was ultrasonicated during 15 min, mechanically stirred further 15 min and dried at room temperature and pressure until complete toluene removal.

2.4. Optical measurements

Absorption spectra were recorded using the spectrophotometer U-2001 Hitachi in scanning ratio 100 nm/min. The absorbance spectrum for sample KAO (KAO-polymer 5) was obtained with a reflection set-up. Photoluminescence (PL) and photoluminescence excitation (PLE) measurements were performed in Shimadzu RF-5301-PC spectrofluorimeter.

The clay/polymer powder was inserted and manually pressed into an orifice of 4 mm diameter and 0.5 mm high on a black painted iron plate. The photophysical experiments were made using the front-face sample orientation due the high light scattering of the powdered material. Care was taken to keep its surface as flat as possible.

The plate was mounted on a goniometer inside the fluorimeter to insure an angle of 45 degrees between the incident excitation beam and the sample. Spectra of solutions were obtained using a 1 cm^2 quartz cuvette.

Steady-state photoluminescence (PL) spectra were recorded from 400 to 800 nm using excitation wavelengths of 390 for solution (Fig. 2a) and thin film samples (Fig. 2b), 400 and 477 nm for clay/polymer composite samples (Fig. 2c and 2d, respectively). Excitation Spectra (PLE) were recorded from 300 to 550 nm using wavelength detection of 465 nm for solution sample (Fig. 2a), 556 nm for thin film sample (Fig. 2b), 500 and 560 nm for clay/polymer samples (Fig. 2c and d, respectively).

2.5. FTIR measurements

LaPPS16 FTIR spectrum was obtained in a BIORAD FTS 3500 GX spectrometer in the range of 400–4000 cm^{-1}, in transmittance mode, LaPPS16 was mixed in 100 mg of KBr. The FTIR spectra of pure-KAO and of KAO/polymer 5 composite where carried out from Nicolet Magna-IR 560 spectrometer, the clay and clay/polymer samples were mixed in 100 mg of KBr.
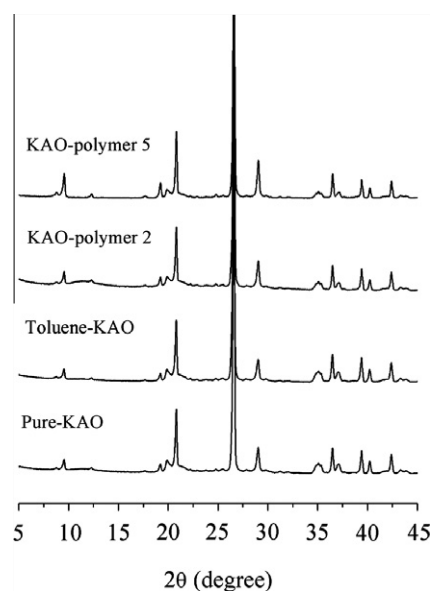

Fig. 1. WAXD diffraction patterns for Pure-KAO, toluene-KAO, KAO-polymer 2, and KAO-polymer 5.
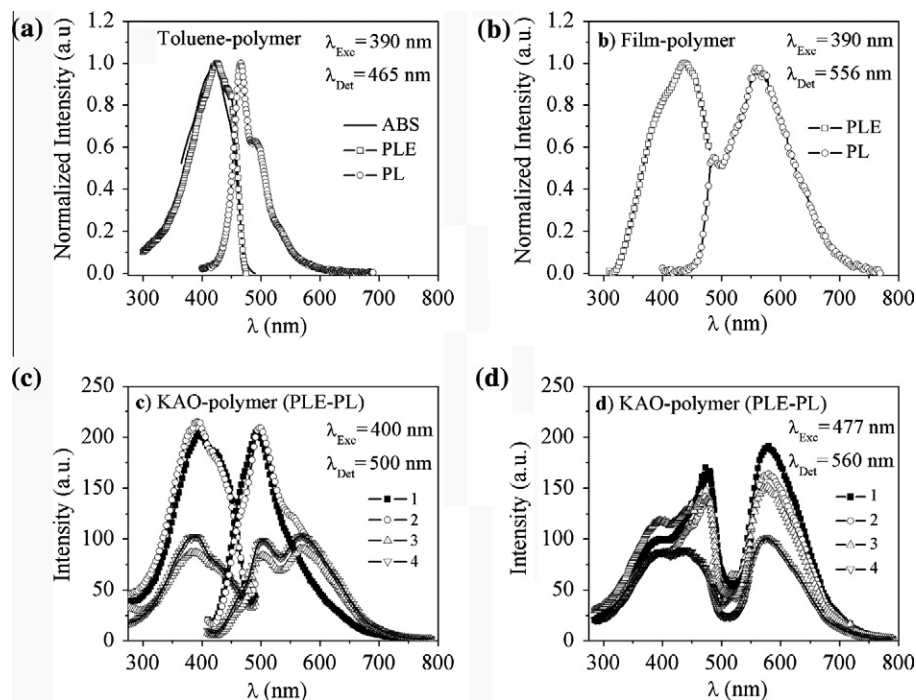
Fig. 2. (a) Optical absorption (ABS), photoluminescence excitation (PLE), and photoluminescence (PL) of the Toluene-polymer sample, (b) PLE and PL spectra of the film-polymer sample. (c) PL (λ_{exc} = 400 nm) and PLE (λ_{em} = 500 nm) spectra of the KAO-polymer 1 (–■– 1), KAO-polymer 2 (–○– 2), KAO-polymer 3 (–Δ– 3) and KAO-polymer 4 (–▽– 4) samples, and (d) PL (λ_{exc} = 477 nm) and PLE (λ_{em} = 560 nm) spectra of the KAO-polymer 1 (–■– 1), KAO-polymer 2 (–○– 2), KAO-polymer 3 (–Δ– 3) and KAO-polymer 4 (–▽– 4) samples.

3. Results and discussion

Fig. 1 shows the WAXD diffractograms obtained for pure-KAO, toluene-KAO, KAO-polymer 2, and KAO-polymer 5, these WAXD diffractograms shows that the kaolinite is the predominant mineral phase which can be identified by its characteristic XRD peaks [30], and minor impurities, such as illite, muscovite, and halloysite, also occur [31].

These patterns show no significant variations, indicating that there is no polymer intercalation within the KAO structure and the interaction clay/polymer occurs most probably on the KAO surfaces.

Fig. 2a shows optical absorption (ABS), photoluminescence excitation (PLE), and photoluminescence (PL) for LaPPS16 in toluene solution at 4.7 µmol L^{-1}. The absorption and excitation spectra are overlapped and centered at 422 nm. With excitation at 390 nm, the PL spectrum showed two-well resolved peaks at 465 nm (zero phonon) and at 493 nm (first phonon), which were attributed to the emission of the isolated chromophore. The absorption/excitation and PL spectra are not mirror images, indicating that energy migration or conformational relaxation from the initial excited state to the lower energy Franck-Condon state are occurring before the emission [4,9,10,27]. We also recorded PLE and PL spectra of the spin coated film of LaPPS16 (Fig. 2b), which showed a broad excitation band centered at 440 nm. The PL spectrum presented a new red-shifted band at 556 nm; this emission can be ascribed as the finger print of the aggregated species. Therefore, we can define two spectral ranges in PLE and PL spectra, correlated with isolated and aggregated species.

The comparison of emission and excitation curves between toluene solutions (Fig. 2a), polymer film (Fig. 2b) and clay/polymer nanocomposite (Fig. 2c and d) clearly demonstrates the dependence on polymer concentration; for lower loading sorption the emission is narrow and blue-shifted (Fig. 2c and d). PL spectra on Fig. 2c present two well-defined peaks: one centered at 500 nm, which relative intensity decreases with increases with the content of the sorbed polymer, and another centered around 560 nm. The comparison of the PL spectrum of the isolated species (Fig. 2a) and that of the aggregated ones (Fig 2b), with the emission spectra of the nanocomposites in Fig. 2c and d lead us to conclude that there are two populations of sorbed polymer chains on the particle surface: isolated and aggregated species. As an additional evidence of de-aggregation dependence on polymer concentration, the excitation spectra acquired using the red-edge excitation at 477 nm (Fig. 2d) showed a relative increase of the aggregate emission as expected, due to the preferential excitation of this population. Moreover, the analysis of PLE spectra in Fig. 2c and d shows that the relative intensity of the excitation band around 390–400 nm is higher for detection at 500 nm (where the emission for isolated species is preferentially expected) and at lower load sorption conditions. The red-shifted band is intensified when higher loading conditions is used or when the excitation is recorded using the red-shifted emission (560 nm). The sharper red-edge excitation peak at 477 nm suggests that

"J" aggregates has been formed [32]. However, the other conditions that should arise from the formation "J" aggregates such as the smaller Stokes shift and the sharper photoluminescence are not as clear as in classical "J" aggregates. It is quite interesting that the excitation spectrum of this ordered species is not observed in film.

The effect of the more drastic sample preparation (KAO-polymer 5) was detected by FT-IR (Fig. 3a). It was observed that the KAO-polymer 5 OH FT-IR spectrum, in the range 3700–3600 cm^{-1}, is narrower and more resolved that the Pure-KAO OH FT-IR spectrum. This result indicates that the more intense sample ultrasonication enhance the separation of the kaolinite agglomerates which form an vermicular structure [30], increasing the clay surface area for polymer sorption and, consequently, increasing the polymer de-aggregation.

Fig. 3b displays normalized PLE in three different emission wavelengths (482, 507, and 550 nm) and the PL spectra in two excitation wavelengths (400 and 445 nm) of KAO-polymer 5 sample. The two PL spectra and the three PLE spectra show the same line shapes typical of the isolated chain, corroborating the condition of polymer de-aggregation. In addition to this conclusion, we can also see that excitation and emission spectra are now mirror images, indicating that the efficiency of energy migration and conformational relaxation of the polymer chain in the electronic excited state are much less efficient and the decay probably comes from the non-relaxed Franck-Condon state, for the sorbed polymer chains.

Analyzing Figs. 2a and 3b, in addition to the red-edge emission in the PL spectra, some spectral shift are also observed, which may result from inner-filter effect or from self-absorption and re-emission process [4]. This effect is more pronounced for more concentrated samples. In order to evaluate the contribution of the self-absorption and re-emission process, we attempted to estimate this contribution throughout Eq. (1) [33,34]:

$$1(\lambda) = I_o(\lambda) \frac{1 - \exp[-A(\lambda)]}{A(\lambda)} \tag{1}$$

$A(\lambda)$ stands for the absorbance curve, $I_0(\lambda)$ for the corrected PL spectrum, and $I(\lambda)$ for the experimental spectrum. Fig. 4 shows the PL spectra (λ_{exc} = 400 nm), $I(\lambda)$ and $I_0(\lambda)$ (Eq. (1)), for LaPPS16 in toluene solution (sample toluene-polymer) and KAO-polymer nanocomposite (sample KAO-polymer 5). The absence of significant self-absorption in both cases indicates that the emitted photons travelling along the optical pathways were not absorbed and re-emitted. It is important to note that the absorbance spectrum for KAO-polymer 5 sample was obtained via reflection set-up, which in general reduces the inner filter effect.

Since the photoluminescent properties of the conjugated polymers strongly depend on the polymer morphology [15–17] and the LaPPS16 has a strong tendency to aggregate [17], through the π-stacking, the changes between the profile seen on Figs. 2c and 3b are due mainly to the de-aggregation of the polymers chain and to the
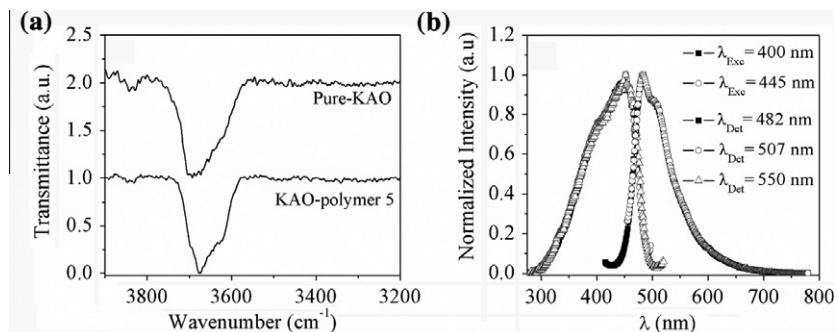
Fig. 3. (a) Pure-KAO and KAO-polymer 5 FTIR spectra in the –OH transition range and (b) PLE and PL spectra for KAO-polymer 5 solid state sample at two different excitation wavelengths 400 and 445 nm and three different emission wavelengths 482, 507, and 550 nm.
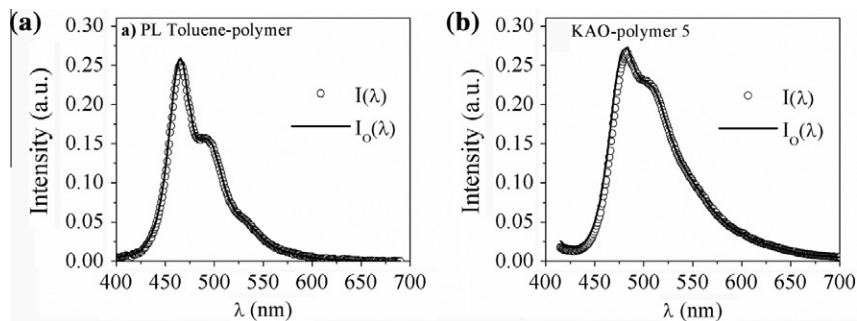

Fig. 4. PL Self-absorption correction for samples (a) toluene-polymer (b) KAO-polymer 5. Open circles refer to experimental data and continuous lines were calculated using both Eq. (1) and experimental absorbance spectra.

combination of the changes on the effective conjugation length and on the conformational distribution of the conjugated polymers due the polymer/clay interaction.

To get additional insights about the interaction clay/polymer, we simulated the emission spectrum for both samples using the electron-phonon coupling model [33,34]. According to this model, the vibronic shape of the emission line may be described considering a multivibrational mode in Frank-Condon approximation, Fermi's golden rule scope, and localized molecular exciton theory [33,34]. Eq. (2) includes the electron-vibrational modes coupling, the Huang-Rhys factor S in pure displacement approach – Eq. (3).

$$I_{ab}(\omega) = \frac{2a_m\pi\omega^3}{3ch}|\vec{\mu}_{ab}|^2 \int_{-\infty}^{+\infty} dt \exp(it(\omega_{ab} - \omega) \\ - \frac{d^2t^2}{2}) \prod_j G_j^*(t) \qquad (2)$$
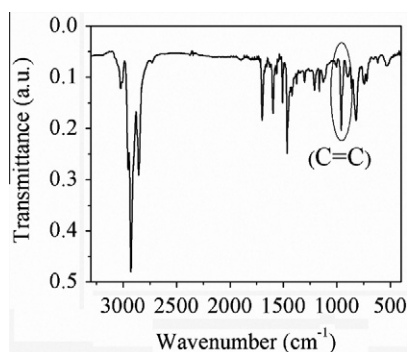

Fig. 5. Pure LaPPS16 FTIR spectrum.

$$G_j^*(t) = \exp[-\sum_{j=1}^{N} S_j\{(\bar{n}_j + 1)\exp(it\omega_j) \\ + \bar{n}_j(\exp(-it\omega_j) - 1)\}] \qquad (3)$$

$\vec{\mu}_{ab}$ stands for the transition electric dipole element, a_m is a constant and which describes the medium effect, c is the speed of light, $\hbar\omega_{ab} = E_b - E_a$ is the energy difference between the localized electronic states LUMO (E_b) and HOMO (E_a), d is the inhomogeneous spectral line width, ω_j is the vibrational mode energy, and $\bar{n}_j = (\exp(\hbar\omega_j/2kT) - 1)^{-1}$ is the thermal occupation probability for the jth-vibrational mode.

The possible vibrational modes, to be coupled, were obtained from the FTIR spectrum of pure LaPPS16 (Fig. 5). The effective vibrational modes v_1, v_2, and v_3 were related to C–H plus C–C ring out-of-plane bending (522 and 555 cm^{-1}), C–H ring in-plane-bending (1005, 1135, and 1174 cm^{-1}), and C–C ring stretching (1518, 1543, 1550, and 1584 cm^{-1}), respectively [35].

Fig. 6 displays the simulated PL spectra calculated from Eqs. (2) and (3) for both samples (toluene-polymer and KAO-polymer 5). The experimental data used in the adjust were: (i) the wavelength of zero phonon transition peak λ_{ab} (462 nm, the pure electronic peak, for toluene-polymer sample and 476 nm for KAO polymer 5 sample), (ii) the zero-phonon inhomogeneous line width d (at half height width of zero-phonon peak), and (iii) three effective vibrational modes: $v_1 = 1550$ cm^{-1}, $v_2 = 1163$ cm^{-1}, and $v_3 = 500$ cm^{-1}. The adjustable parameters S_j, where $j = 1$, 2, and 3, are the electron-vibrational modes coupling parameter, i.e., the Huang-Rhys factors. Table 2 displays the list of the parameters used in the PL line shape adjusting for both spectra. Observing the final results in Table 1 for KAO-polymer 5 sample, in comparison with toluene-polymer sample, the line shape width does not increase
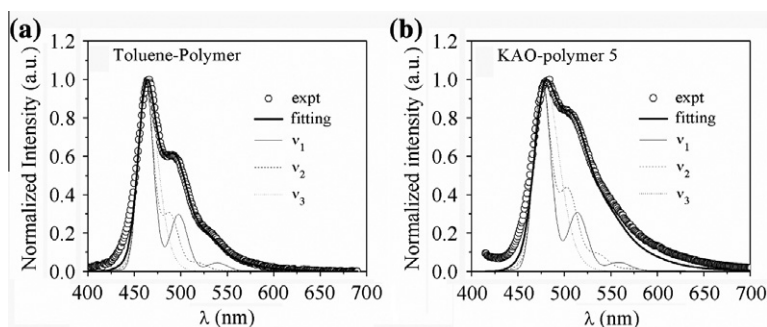

Fig. 6. Experimental (open circles) and theoretical fitting (solid line) of normalized PL spectra for (a) toluene-polymer and (b) KAO-polymer 5 samples. The contributions of each phonon, $v_1 = 1550$ cm^{-1}, $v_2 = 1163$ cm^{-1}, and $v_2 = 500$ cm^{-1} are presented.

Table 2
Theoretical adjusting parameters of PL spectra for toluene-polymer and KAO-polymer 5 samples.

Sample	λ_{ab} (nm)	d (cm^{-1})	$v_1 = 1550$ cm^{-1}	$v_2 = 1163$ cm^{-1}	$v_3 = 500$ cm^{-1}
Toluene-polymer	462	380	$S_1 = 0.3$	$S_2 = 0.3$	$S_3 = 0.3$
KAO-polymer 5	476	400	$S_1 = 0.3$	$S_2 = 0.4$	$S_3 = 0.6$

substantially. However, the parameter S_3, effective vibrational mode at $500\,cm^{-1}$, rises significantly. Thus, the interaction clay/polymer does not introduce large molecular disorder, the line width d is similar, and is greater in the aromatic ring regions. Even though the PL spectrum is red shifted, the theoretical result agrees with the PLE and selective PL emission experiments presented in Fig. 3b confirming the de-aggregation of LaPPS16 on clay nanosubstrates.

4. Conclusions

The de-aggregation of a very luminescent polyfluorene derivative poly(9,9-di-hexylfluorenediyl divinylene-*alt*-1,4-phenylenevinylene) (LaPPS16), which has a high tendency to π-stacking aggregation, was achieved through the preparation of the polymer/clay nanocomposites. The sonicated and mechanically stirred mixture of diluted toluene solution of the polymer with non-treated KAO was enough to promote its de-aggregation through the polymer adsorption on the clay surfaces, being the de-aggregation more efficient under stronger sonication/stirring conditions. The results presented in this report bring the possibility of producing more efficient polymer based luminescent devices and to carry single-molecule studies using nanocomposite film formation.

References

[1] Hide F, DiazGarcia MA, Schwartz BJ, Heeger AJ. New developments in the photonic applications of conjugated polymers. Acc Chem Res 1997;30(10):430–6.
[2] Leclerc M. Polyfluorenes: twenty years of progress. J Polym Sci Pol Chem 2001;39(17):2867–73.
[3] Akcelrud L. Electroluminescent polymers. Prog Polym Sci 2003;28(6):875–962.
[4] Grimsdale AC, Chan KL, Martin RE, Jokisz PG, Holmes AB. Synthesis of light-emitting conjugated polymers for applications in electroluminescent devices. Chem Rev 2009;109:897–1091.
[5] Inganäs O, Zhang F, Tvingstedt K, Andersson LM, Hellström S, Andersson MR. Polymer photovoltaics with alternating copolymer/fullerene blends and novel device architectures. Adv Mater 2010;22:100–16.
[6] Svanström CM B, Rysz J, Bernasik A, Budkowski A, Zhang F, Inganäs O, et al. Device Performance of APFO-3/PCBM Solar Cells with Controlled Morphology. Adv Mater 2009;21:4398–403.
[7] Müller C, Wang E, Andersson LM, Tvingstedt K, Zhou Y, Andersson MR, et al. Influence of molecular weight on the performance of organic solar cells based on a fluorene derivative. Adv Funct Mater 2010;20:1–8.
[8] Zhao D, Tang W, Ke L, Tan ST, Sun XW. Efficient bulk heterojunction solar cells with poly[2,7-(9,9-dihexylfluorene)-alt-bithiophene] and 6,6-phenyl C6 l butyric acid methyl ester blends and their application in tandem cells. Appl Mater Interfaces 2010;2(3):877–87.
[9] Monkman A, Roth C, King S, Dias F. In: Scherf U, Neher D, editors. Polyfluorenes, advances in polymer science, vol. 212. Berlin: Springer-Verlag; 2008. p. 187–225.
[10] Knaapila M, Winokur MJ. In: Scherf U, Neher D, editors. Polyfluorenes, advances in polymer science, vol. 212. Berlin: Springer-Verlag, p. 227–72.
[11] Nowacki B, Iamazaki E, Cirpan A, Karasz F, Atvars TDZ, Akcelrud L. Highly efficient polymer blends from a polyfluorene derivative and PVK for LEDs. Polymer 2009;50:6057–64.
[12] Mirzov O, Scheblykin IG. Photoluminescence spectra of a conjugated polymer: from films and solutions to single molecules. Phys Chem Chem Phys 2006;8(47):5569–76.
[13] Becker K, Lupton JM. Efficient light harvesting in dye-endcapped conjugated polymers probed by single molecule spectroscopy. J Am Chem Soc 2006;128(19):6468–79.
[14] Odoi MY, Hammer NI, Rathnayake HP, Lahti PM, Barnes MD. Single-molecule studies of a model fluorenone. ChemPhysChem 2007;8(10):1481–6.
[15] Telbiz GM, Posudievsky OY, Dementjev A, Kiskis J, Gulbinas V, Valkunas L. Effect of nanoscale confinement on fluorescence of MEH-PPV/MCM-41 composite. Phys Status Solid A 2010;207(9):2174–9.
[16] Lin H, Hania RP, Bloem R, Mirzov O, Thomsson D, Scheblykin IG. Single chain versus single aggregate spectroscopy of conjugated polymers. Where is the border? Phys Chem Chem Phys 2010;12:11770–7.
[17] Tozoni JR, Guimarães FEG, Atvars TDZ, Nowacki B, Akcelrud L, Bonagamba TJ. De-aggregation of polyfluorene derivative by blending with a series of poly(alkyl methacrylate)s with varying sidegroup sizes. Euro Polym J 2009;45(8):2467–77.
[18] Akcelrud L, Simas ER, Glogauer A, Gehlen M. Excited state dynamics of polyfluorene derivatives in solution. J Phys Chem A Mol Spectrosc Kinet Environ General Theor 2008;112:5054–9.
[19] Theng BKG. Formation and properties of clay–polymer complexes. Amsterdam: Elsevier; 1979.
[20] Ogawa M, Kuroda K. Photofunctions of intercalation compounds. Chem Rev 1995;95:399–438.
[21] Eckle M, Decher G. Tuning the performance of Layer-by-Layer Assembled Organic Light Emitting Diodes by controlling the position of isolating clay barrier sheets. Nano Lett 2001;1(1):45–9.
[22] Lee HC, Lee TW, Lim YT, Park OO. Improved environmental stability in poly(*p*-phenylene vinylene)/layered silicate nanocomposite. Appl Clay Sci 2002;21:287–93.
[23] Schoonheydt RA. Smectite-type clay minerals as nanomaterials. Clays Clay Miner 2002;50(4):411–20.
[24] Ramachandran G, Simon GP, Cheng YB, Dai L. Control of fluorescence emission color of benzo 15-crown-5 ether substituted oligo phenylene vinylene-ceramic nanocomposites. Polymer 2005;46:7176–84.
[25] Jing C, Chen L, Shi Y, Xigao J. Synthesis and characterization of exfoliated MEH-PPV/clay nanocomposites by in situ polymerization. Euro Polym J 2005;41:2388–94.
[26] Cossiello RF, Susman MD, Aramendia PF, Atvars TDZ. Study of solvent-conjugated polymer interactions by polarized spectroscopy: MEH–PPV and Poly(9,90-dioctylfluorene-2,7-diyl). J Lumin 2010;130:415–23.
[27] Kasha M, Rawls HR, El-Bayoumi MA. The exciton model in molecular spectroscopy. Pure Appl Chem 1965;11:371.
[28] Schumacher S, Galbraith I. Dynamics of photoexcitation and stimulated optical emission in conjugated polymers: a multiscale quantum-chemistry and Maxwell-Bloch-equations approach. Phys Rev B 2010;81:245407.
[29] Pankove JI. Optical process in semiconductors. New York: Dove Publications; 1975.
[30] Zhao H, Deng Y, Harsh JB, Flury M, Boyle JS. Alteration of kaolinite to cancrite and sodalite by simulated hanford tank waste and its impact on cesium retention. Clays Clay Miner 2004;52(1):1–13.
[31] Reyes CAR, Williams CD. Hydrothermal transformation of kaolinite in the system $K_2OSiO_2Al_2O_3H_2O$. DYNA 2010;163(77):55–63.
[32] Jelley EE. Spectral Absorption and Fluorescence of Dyes in the Molecular State. Nature 1936;138:1009–10.
[33] Chang R, Hsu JH, Fann WS, Liang KK, Chang CH, Hayashi M, et al. Experimental and theoretical investigations of absorption and emission spectra of the light-emitting polymer MEH-PPV in solution. Chem Phys Lett 2000;317:142.
[34] Marletta A, Guimarães FEG, Faria RM. Braz J Phys 2002;32:570.
[35] Voss KF, Foster CM, Smilowitz L, Mihailović D, Askari S, Srdanov G, et al. Substitution effects on bipolarons in alkoxy derivatives of poly(1,4-phenylene-vinylene). Phys Rev B 1991;43:5109–18.

MACROMOLECULAR NANOTECHNOLOGY